Lithuanian Journal of Physics
Vol. **66**, No. 1, pp. 48–60 (2026)
ISSN 1648-8504 eISSN 2424-3647
DOI: https://doi.org/10.3952/physics.2026.66.1.6

EXPERIMENTAL (RAMAN AND IR) AND COMPUTATIONAL (DFT) STUDIES OF THE CYCLOHEXYLTRIFLUOROSILANE

J. Mačytė [a], J. Lach [a], M. Gregory [b], S. Gordon [b], J. Čeponkus [a], V. Šablinskas [a], and G.A. Guirgis [b]

[a] *Faculty of Physics, Vilnius University, Saulėtekio 9, 10222 Vilnius, Lithuania*
[b] *Department of Chemistry and Biochemistry, College of Charleston, Charleston, SC 29424, USA*
Email: valdas.sablinskas@ff.vu.lt

Received 1 December 2025; accepted 21 January 2026

This study presents an experimental (Raman and IR spectroscopy) and computational (DFT) investigation of cyclohexyltrifluorosilane to identify its stable conformers and assign its experimental vibrational spectral bands. Computational analysis confirmed the existence of two stable chair conformers: chair equatorial (most stable) and chair axial. The potential energy difference between these conformers was found to be 6.3 kJ/mol, and the interconversion barrier was determined to be too high to overcome it at matrix experiments conditions. To provide a complete assignment of the compound's vibrational spectral bands, experimental data from ATR-FTIR, Raman, and matrix isolation IR spectroscopy were used in conjunction with DFT calculations. The experimental results confirm the existence of only one conformer in the chair equatorial configuration.

Keywords: cyclohexyltrifluorosilane, matrix isolation, infrared spectroscopy, Raman spectroscopy, conformational analysis, DFT, B3LYP, cc-pVTZ

1. Introduction

Organosilicon cyclic compounds hold promise as surface modification coatings due to their excellent surface adhesion properties [1]. The incorporation of a silicon atom into the cyclic ring enhances adhesion through covalent bonding with glass. Furthermore, substituting the ring's hydrogen atoms with radicals, such as halogen atoms or methyl groups, improves hydrophobic properties [2, 3]. This effect is influenced by the ring size, the type of substituents, and the molecule's conformational diversity.

Therefore, conformational analysis is critical for understanding the chemistry and spectroscopic features of heterocyclic organic molecules [4]. The dynamics and pathways of conformational rearrangements significantly impact molecular properties, including chemical and biological activity. Importantly, even small radical substitutions can profoundly affect these properties [5, 6].

The stability of substituted cyclohexanes depends on factors like steric hindrance, 1,3-diaxial interactions, and electronic effects. Cyclohexane primarily adopts chair conformation, which minimizes strain. In this conformation, substituents can occupy either axial or equatorial positions, and their position determines the stability of the molecule. Substituents in the equatorial position experience fewer steric interactions than those in the axial position. This is because axial substituents interact unfavourably with the two hydrogen atoms on the same side of the ring (1,3-diaxial interactions). Larger substituents prefer the equatorial position to minimize steric interactions, making the molecule more stable [7–10].

When a substituent is in an axial position, it interacts with the hydrogens in the 1,3 positions (on the same side of the ring). This increases the energy of the conformation, leading to decreased stability.

The larger the substituent, the greater the steric hindrance when in the axial position. Thus, bulkier groups (e.g. tert-butyl or isopropyl) strongly prefer the equatorial position [11].

Electronegative substituents like halogens or groups capable of hydrogen bonding may have an impact on stability due to inductive or electronic

effects. For example, an electronegative atom like fluorine might stabilize certain conformations because it withdraws electron density from the ring.

2. Methodology

Cyclohexyltrifluorosilane was prepared at the College of Charleston during research into novel hydrophobic coatings. The present study is an analysis of cyclohexyltrifluorosilane through a combination of vibrational spectroscopy and theoretical calculations.

Conformational analysis of the chair and boat conformers was performed using Gaussian at the B3LYP/cc-pVTZ theory level. Harmonic and anharmonic frequency analyses were also conducted at this same level of theory [12–14].

The vibrational mode automatic relevance determination (VMARD) method was used to describe computationally predicted normal vibrational modes obtained with the B3LYP/cc-pVTZ method. The automatic relevance determination (ARD) method for Bayesian ridge regression was used since it gives a good estimation of the most prominent internal coordinates analysis [15].

Infrared absorption spectra of the liquid sample were recorded using a *Bruker* Alpha spectrometer with a single reflection diamond accessory, a globar source, and a DTGS (deuterated L – alanine doped triglycerine sulphate) detector. The attenuated total reflection (ATR) method was employed. Due to the significant sample evaporation during the measurement, 64 scans were acquired at 4 cm^{-1} resolution.

Raman spectra of the compound were acquired using a *Bruke*r MultiRAM FT-Raman spectrometer (*Bruker Optik GmbH*, Ettlingen, Germany). A 1064 nm Nd:YAG laser served as the excitation source, and a liquid nitrogen-cooled germanium diode was employed as the detector. Measurements were conducted with a laser power of 1000 mW, a resolution of 4 cm^{-1}, and involved averaging 128 spectra.

Matrix isolated samples were prepared in a conventional vacuum system. The liquid sample underwent a freeze-pump-thaw cycle for degassing and was then mixed with host gases (argon and nitrogen). The mixture was prepared by combining 0.1 mbar of vapourized cyclohexyltrifluorosilane with 1000 mbar of the matrix gas in the same volume. This mixture was subsequently deposited onto a CsI window cooled to 19 K (for argon and nitrogen) within a closed-cycle (Janis SHI-4) cryostat (operating temperature range: 3–300 K). During experiments, a *Bruker* IFS 120 spectrometer (*Bruker Optik GmbH*, Ettlingen, Germany) was used, employing a KBr beamsplitter, a globar source, and an MCT detector, with a resolution of 1 cm^{-1}. For each measurement, 256 spectra were averaged. Annealing of the matrix was carried out at 35 K for the nitrogen and argon matrix. The selection of annealing temperatures was based on the understanding that exceeding those temperatures could lead to intense matrix evaporation, potentially damaging the matrix structure and causing irreversible changes.

3. Results and discussion

3.1. Computation

A conformational analysis of the cyclohexyltrifluorosilane molecule was performed to identify the stable conformers, transition states, and possible interconversion pathways. As initial structures, the most probable chair, boat, and skew-boat ring shapes with the substituent in axial and equatorial positions were chosen for the geometry optimization. The detailed investigation of the conformational landscape confirmed the existence of two stable conformers (see Fig. 1). These consist of the ring in a chair shape with the trifluorosilane substituent in either axial or equatorial position. The cyclohexyltrifluorosilane molecule is most stable in the chair equatorial conformation, with the chair axial conformation representing a local energy minimum. The relative energy difference between those conformers was found to be 6.3 kJ/mol.

To check the conformational stability, the relaxed potential energy surface scan was done for the chair equatorial to chair axial conformation via ring inversion. The energy change was traced along with the C_6–C_1–C_2–C_3 dihedral angle change about 5 deg, and the structure was optimized at every step (every dihedral angle change). The results indicate that the chair equatorial to chair axial interconversion energy barrier is equal to 46.3 kJ/mol (see Fig. 2). The reverse process, the chair axial to chair equatorial energy barrier is 18.9 kJ/mol through the skew-boat ring conformation, making both

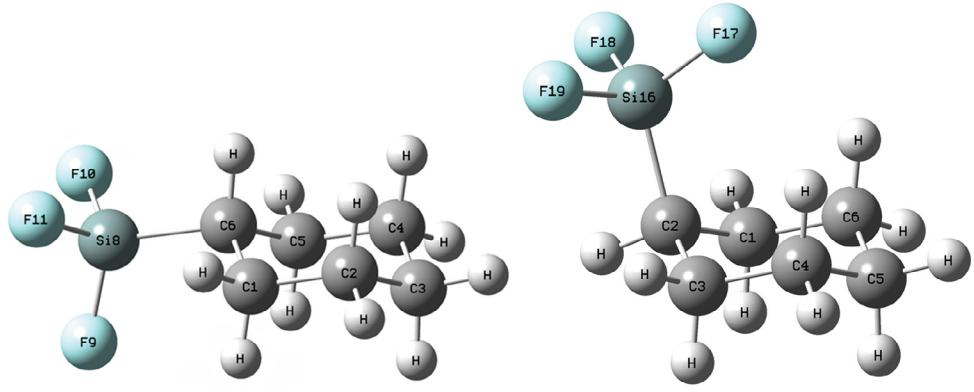

ΔE = 0 kJ/mol ΔE = 6.3 kJ/mol

Fig. 1. The chair equatorial and chair axial conformers of cyclohexyltrifluorosilane with atoms numbering from DFT/B3LYP/cc-pVTZ calculations.

processes unobservable in the matrix isolation experimental conditions.

To make a detailed assignment of the experimental vibrational modes, a VMARD analysis was performed for the global energy minimum structure: the chair equatorial conformer. An internal coordinate (S) list is provided in the section 'Experimental results', in Table 2.

Vibrational analysis was performed utilizing DFT/B3LYP/cc-pVTZ for harmonic approximation and anharmonic approximation. VMARD analysis was done for the results obtained from the DFT/B3LYP/cc-pVTZ method (see Table 3).

The VMARD analysis revealed that the potential energy of normal vibrations was very dissipated in the fingerprint spectral range of 1000–1400 cm^{-1}. This result is not common for conventional organic compounds containing mainly carbon, oxygen, nitrogen and hydrogen. The title compound is different since it also contains very electronegative

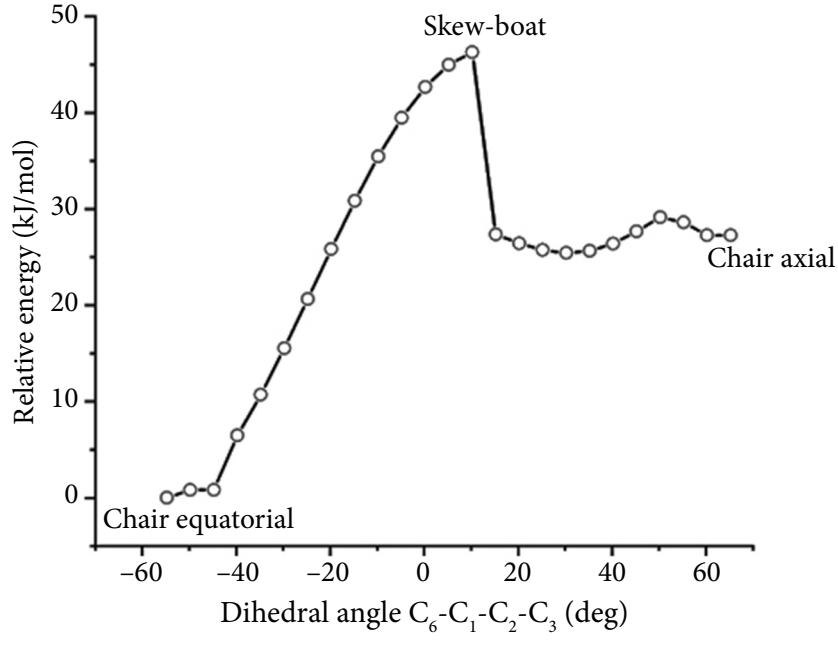

Fig. 2. Relaxed potential energy surface scan for the chair equatorial to chair axial interconversion obtained from the DTF/B3LYP/cc-pVTZ. The energy values are presented with respect to the energy value of the lowest conformer for each relaxed surface scan.

fluorine atoms as well as a heavy silicon atom. This circumstance is the reason that a large number of deformational vibrational modes and stretching modes involving the heavy atom fall into the narrow spectral 1000–1400 cm^{-1} range and cause a very high dissipation of vibrational potential energy.

Based on the previous calculations, it was shown that the DFT/B3LYP/cc-pVTZ method properly describes the conformational stability of the heterocyclic molecules.

3.2. Experiment

In addition to the structural analysis of cyclohexyltrifluorosilane, this study aims, for the first time, to provide a complete assignment of the vibrational spectral bands of this compound. We used several spectroscopic methods for the analysis of the conformational variety of the cyclohexyltrifluorosilane molecule. The ATR-FTIR spectrum, along with the calculated spectra of the two conformers, is presented in Fig. 3 (left panel). Theoretical calculations indicate that the bands of the chair axial conformer do not exhibit any vibrational mode that can be identified through experimental means for this conformer.

The Raman spectrum of the cyclohexyltrifluorosilane molecule along with the calculated spectra for two analyzed conformers is depicted in Fig. 3 (right panel). Since the width of the ATR-FTIR absorption and Raman spectral bands of the liquid sample is in a range of 20–25 cm^{-1}, only the general assignment of the bands to the normal vibrations can be made. Additionally, the calculations performed in harmonic approximation (see Table 1) do not take into account the anharmonicity of potential functions of the normal vibrations.

The width of these bands can be attributed to two primary factors: temperature and intermolecular interactions. Proceeding with spectroscopic experiments in a condensed (liquid or solid) state at ambient temperatures does not allow one to eliminate intermolecular interactions and this makes the vibrational spectral bands broader. In order to reduce the width of the experimental vibrational spectral bands, the spectroscopic experiments should be performed on molecules isolated in an inert medium at very low temperatures with suppressed intermolecular interactions.

Matrix isolation FTIR studies were employed for a more detailed conformational analysis. The matrix isolation spectra of cyclohexyltrifluorosilane are presented in Fig. 4. According to the calculated potential energy surface of the title compound, the most stable conformer is the chair equatorial. The energy difference between the chair equatorial and chair axial conformers was found to be 6.3 kJ/mol, and the energy barrier for an interconversion via ring inversion from chair axial to chair equatorial 18.9 kJ/mol, making this process unfavoured in experimental conditions. The chair axial conformer is the higher energy form and based on the B3LYP energy difference between the chair axial and chair equatorial conformers, its population at room temperature (calculated using the Boltzmann distribution) should be approximately 1:12. Thus, for each molecule in the chair axial form, about 12 molecules are in the chair equatorial form. In the experimental spectrum, we did not find any argument (characteristic vibrational modes) to support the need

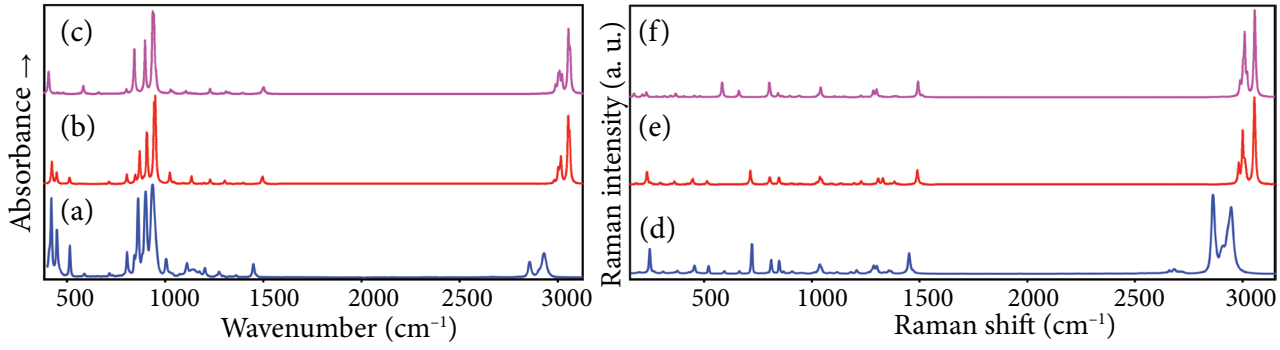

Fig. 3. (a) ATR-FTIR absorption spectrum of cyclohexyltrifluorosilane, together with the theoretical DFT/B3LYP/cc-pVTZ calculated IR absorption spectra of the (b) equatorial and (c) axial conformations; (d) Raman spectrum of cyclohexyltrifluorosilane, together with the theoretical DFT/B3LYP/cc-pVTZ calculated Raman spectra of the (e) equatorial and (f) axial conformations.

Table 1. Experimental measurements using ATR and Raman spectroscopy, combined with calculations performed using the B3LYP/-cc-pVTZ method, were used to study the vibration modes of a cyclohexyltrifluorosilane molecule in the equatorial and axial conformations.

Experimental				Calculated					
				DFT B3LYP/cc-pVTZ					
				Equatorial			Axial		
Freq, cm^{-1}	IR *I*, arb. u.	Freq, cm^{-1}	Raman *I*, arb. u.	Freq, cm^{-1}	IR *I*, arb. u.	Raman *I*, arb. u.	Freq, cm^{-1}	IR *I*, arb. u.	Raman *I*, arb. u.
				3061	47	3	**3063**	52	9
2930	27	**2940**	84	**3058**	12	28	**3058**	4	35
				3055	9	90	**3056**	16	100
2905	9	**2905**	16	**3053**	37	65	**3054**	50	1
				3052	41	21	**3053**	24	23
							3021	17	16
							3020	7	13
				3016	33	13			
				3013	0.2	12			
2857	17	**2857**	100	**3010**	9	23	**3009**	26	95
				3003	14	2	**3003**	10	3
				3001	6	100	**3002**	13	34
							2988	11	20
				2982	4	39			
		2710	3						
		2677	3						
		2654	3						
							1513	1	1
				1510	1	0.4			
							1503	7	0.1
1149	14	**1447**	26	**1497**	7	0.4	**1498**	5	0.2
				1493	3	1	**1494**	0.1	5
				1491	2	4	**1492**	2	4
				1489	0.3	6			
1362	3	**1362**	4	**1397**	2	0.3	**1395**	1	0.3
							1389	0.3	0.2
							1387	0.1	0.1
				1384	0.1	2			
				1383	0.1	0.3			
							1381	0.001	0.4
				1374	0.1	0.1			
		1352	4						
1330	2	**1330**	1	**1366**	0.4	1	**1359**	0.1	0.001
1296	2	**1296**	10	**1330**	0.4	4	**1326**	2	0.3
		1282	10						
				1308	0.1	3			
1274	6			**1304**	5	0.4	**1310**	4	0.2

Table 1. (Continued)

Experimental				Calculated					
				DFT B3LYP/cc-pVTZ					
				Equatorial			Axial		
Freq, cm^{-1}	IR *I*, arb. u.	Freq, cm^{-1}	Raman *I*, arb. u.	Freq, cm^{-1}	IR *I*, arb. u.	Raman *I*, arb. u.	Freq, cm^{-1}	IR *I*, arb. u.	Raman *I*, arb. u.
							1300	0.1	4
1260^{sh}	2	**1260^{sh}**	1	**1288**	0.3	0.1	**1286**	1	3
1203	11	**1203**	5	**1229**	6	2	**1229**	7	1
1175	2	**1176**	1	**1197**	2	1			
							1150	1	0.2
							1128	1	0.1
1111	9	**1112**	1	**1135**	11	1			
							1106	4	0.3
1075	2	**1076**	1	**1094**	1	0.2	**1095**	1	0.003
				1088	0.2	0.3			
							1042	0.5	2
1035	2	**1031**	12	**1046**		2	**1040**	3	2
				1037	0.3	3			
1005	16	**1006**	1	**1024**	16	1	**1028**	6	1
							953	17	0.03
936	100	**940**	1	**950**	100	0.2	**943**	95	0.4
				943	86	0.2	**936**	100	0.2
				925	1	0.04			
900	92	**903**	3	**907**	70	0.5	**898**	79	0.4
880^{sh}	5			**890**	4	0.1			
862	86	**863**	3	**870**	45	0.1	**863**	0.5	0.01
							861	0.3	0.3
843	3	**843**	16	**847**	11	2	**843**	67	1
							803	0.01	0.2
806	27	**806**	18	**805**	13	2	**802**	6	4
				797	0.2	0.2			
716	5	**716**	37	**714**	3	4			
659	2	**659**	3				**661**	2	1
588	5	**589**	3				**583**	12	3
514	34	**515**	10	**513**	9	1			
							480	1	0.2
							454	1	0.2
448	52	**449**	10	**447**	16	1			
				443	0.1	0.3			
420	86	**421**	1	**423**	31	0.1			
							406	33	0.1

Note: arb. u. means arbitrary units.

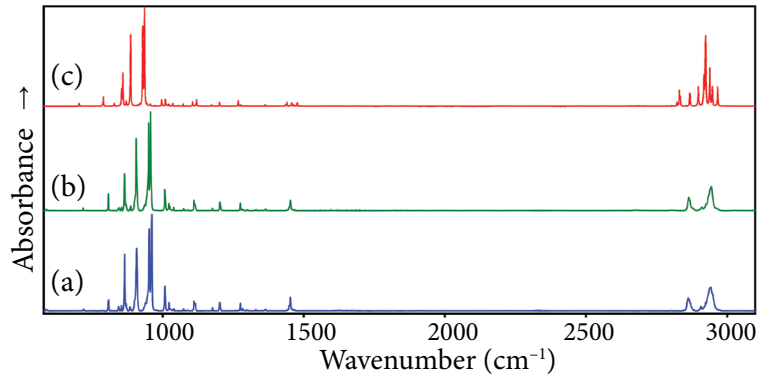

Fig. 4. Infrared absorption spectra of cyclohexyltrifluorosilane isolated in (a) argon at 3 K and (b) nitrogen at 3 K, together with the B3LYP/cc-pVTZ calculated anharmonic IR spectrum of the equatorial conformer.

for the second conformer (chair axial) to explain the observed spectral bands.

Two different matrix gases were used – argon and nitrogen. Some molecules interact differently with argon and nitrogen, so their conformational equilibrium depends on the matrix. One conformer may be more stabilized in argon, while another is found to be more stable in nitrogen. Conformers with a large dipole moment are stabilized in more polar matrices like nitrogen, but non-polar or symmetric conformers are stabilized in non-polar matrices such as argon. Conformers may have vibrational bands that are stronger or weaker in the spectra. The argon matrix was deposited at 19 K, and the nitrogen matrix was prepared at the same temperature.

One of supporting arguments for the existence of chair equatorial conformation is the matrix annealing experiment. After annealing, the relative intensity of the spectral bands should increase because the conformational thermodynamic equilibrium at 300 K in the freshly deposited matrix shifts to the equilibrium at 19 K (in both argon and nitrogen matrices). The annealing results are presented in Fig. 5. The annealing experiments were carried out under the same temperature conditions in both matrices. Figure 5 shows the spectra of the matrix deposited at 19 K and cooled to 3 K, as well as the spectra after annealing from 35 K back down to 3 K.

The spectra of cyclohexyltrifluorosilane isolated in argon and nitrogen matrices before and after annealing match, indicating that no conformational transitions or molecular complex formation happen during the annealing process. This result confirms that only one conformer (chair equatorial) is present in the experiment.

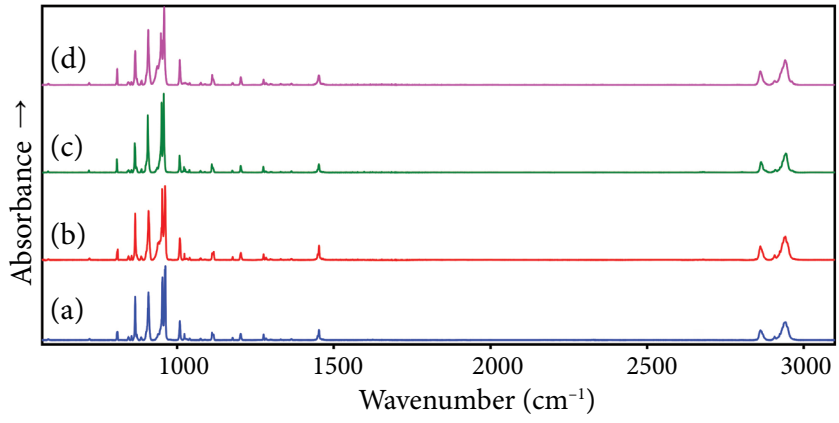

Fig. 5. Infrared absorption spectra of cyclohexyltrifluorosilane isolated in (a) argon at 19 to 3 K and after annealing in (b) argon matrix at 35 to 3 K, together with the spectra recorded in (c) nitrogen matrix at 19 to 3 K and after annealing in (d) nitrogen matrix at 35 to 3 K.

The experimental and calculated infrared absorption bands for the chair equatorial conformer, along with the spectral bands assigned to the fundamental vibrations using vibrational mode automatic relevance determination VMARD, are summarized in Table 3. The calculated vibrational frequencies from the ORCA output were used as input parameters for the vibAnalysis software [15], and VMARD analysis was subsequently performed. A list of internal coordinates (S) is provided in Table 2. Each normal vibration consists of many internal vibrations, so only a significant input to potential energy is used to describe the normal vibrations.

Table 2. Symmetry coordinates used for the description of the normal vibrational modes of cyclohexyltrifluorosilane.

S1 BOND C1 C2	S43 ANGLE C3 C4 H14	S85 TORSION C1 C6 C5 C4
S2 BOND C1 C6	S44 ANGLE C3 C4 H15	S86 TORSION C1 C6 C5 H12
S3 BOND C1 H20	S45 ANGLE H16 C3 H17	S87 TORSION C1 C6 C5 H13
S4 BOND C1 H21	S46 ANGLE C5 C4 H14	S88 TORSION C1 C6Si8 F9
S5 BOND C2 C3	S47 ANGLE C5 C4 H15	S89 TORSION C1 C6Si8 F10
S6 BOND C2 H18	S48 ANGLE C4 C5 C6	S90 TORSION C1 C6Si8 F11
S7 BOND C2 H19	S49 ANGLE C4 C5 H12	S91 TORSION H18 C2 C3 C4
S8 BOND C3 C4	S50 ANGLE C4 C5 H13	S92 TORSION H18 C2 C3 H16
S9 BOND C3 H16	S51 ANGLE H14 C4 H15	S93 TORSION H18 C2 C3 H17
S10 BOND C3 H17	S52 ANGLE C6 C5 H12	S94 TORSION H19 C2 C3 C4
S11 BOND C4 C5	S53 ANGLE C6 C5 H13	S95 TORSION H19 C2 C3 H16
S12 BOND C4 H14	S54 ANGLE C5 C6 H7	S96 TORSION H19 C2 C3 H17
S13 BOND C4 H15	S55 ANGLE C5 C6Si8	S97 TORSION C2 C3 C4 C5
S14 BOND C5 C6	S56 ANGLE H12 C5 H13	S98 TORSION C2 C3 C4 H14
S15 BOND C5 H12	S57 ANGLE H7 C6Si8	S99 TORSION C2 C3 C4 H15
S16 BOND C5 H13	S58 ANGLE C6Si8 F9	S100 TORSION H16 C3 C4 C5
S17 BOND C6 H7	S59 ANGLE C6Si8 F10	S101 TORSION H16 C3 C4 H14
S18 BOND C6Si8	S60 ANGLE C6Si8 F11	S102 TORSION H16 C3 C4 H15
S19 BONDSi8 F9	S61 ANGLE F9Si8 F10	S103 TORSION H17 C3 C4 C5
S20 BONDSi8 F10	S62 ANGLE F9Si8 F11	S104 TORSION H17 C3 C4 H14
S21 BONDSi8 F11	S63 ANGLE F10Si8 F11	S105 TORSION H17 C3 C4 H15
S22 ANGLE C2 C1 C6	S64 TORSION C6 C1 C2 C3	S106 TORSION C3 C4 C5 C6
S23 ANGLE C2 C1 H20	S65 TORSION C6 C1 C2 H18	S107 TORSION C3 C4 C5 H12
S24 ANGLE C2 C1 H21	S66 TORSION C6 C1 C2 H19	S108 TORSION C3 C4 C5 H13
S25 ANGLE C1 C2 C3	S67 TORSION C2 C1 C6 C5	S109 TORSION H14 C4 C5 C6
S26 ANGLE C1 C2 H18	S68 TORSION C2 C1 C6 H7	S110 TORSION H14 C4 C5 H12
S27 ANGLE C1 C2 H19	S69 TORSION C2 C1 C6Si8	S111 TORSION H14 C4 C5 H13
S28 ANGLE C6 C1 H20	S70 TORSION H20 C1 C2 C3	S112 TORSION H15 C4 C5 C6
S29 ANGLE C6 C1 H21	S71 TORSION H20 C1 C2 H18	S113 TORSION H15 C4 C5 H12
S30 ANGLE C1 C6 C5	S72 TORSION H20 C1 C2 H19	S114 TORSION H15 C4 C5 H13
S31 ANGLE C1 C6 H7	S73 TORSION H21 C1 C2 C3	S115 TORSION C4 C5 C6 H7
S32 ANGLE C1 C6Si8	S74 TORSION H21 C1 C2 H18	S116 TORSION C4 C5 C6Si8
S33 ANGLE H20 C1 H21	S75 TORSION H21 C1 C2 H19	S117 TORSION H12 C5 C6 H7
S34 ANGLE C3 C2 H18	S76 TORSION C1 C2 C3 C4	S118 TORSION H12 C5 C6Si8
S35 ANGLE C3 C2 H19	S77 TORSION C1 C2 C3 H16	S119 TORSION H13 C5 C6 H7
S36 ANGLE C2 C3 C4	S78 TORSION C1 C2 C3 H17	S120 TORSION H13 C5 C6Si8
S37 ANGLE C2 C3 H16	S79 TORSION H20 C1 C6 C5	S121 TORSION C5 C6Si8 F9
S38 ANGLE C2 C3 H17	S80 TORSION H20 C1 C6 H7	S122 TORSION C5 C6Si8 F10
S39 ANGLE H18 C2 H19	S81 TORSION H20 C1 C6Si8	S123 TORSION C5 C6Si8 F11
S40 ANGLE C4 C3 H16	S82 TORSION H21 C1 C6 C5	S124 TORSION H7 C6Si8 F9
S41 ANGLE C4 C3 H17	S83 TORSION H21 C1 C6 H7	S125 TORSION H7 C6Si8 F10
S42 ANGLE C3 C4 C5	S84 TORSION H21 C1 C6Si8	S126 TORSION H7 C6Si8 F11

The analysis of the observed absorption bands will first focus on the most intense group of bands, located at 970–850 cm^{-1}. In the range between 970–920 cm^{-1} in both argon and nitrogen matrices, we observe two high-intensity bands. The first band observed in this region, which is also the most intense band, is at 957.8 cm^{-1} in the nitrogen matrix and 960.8 cm^{-1} in the argon matrix. This band was assigned to the Si–F(10) + Si–F(11) stretching vibration. The second, medium-intensity band is located at 950.9 cm^{-1} in the nitrogen matrix and at 952.7 cm^{-1} in the argon matrix. This band is assigned to the Si–F(9) + Si–F(10) + Si–F(11) stretching vibration. Another medium-intensity band group is located at 906–908 cm^{-1} in both matrices and is assigned to the Si–C(6) stretching vibration. The last band in this region is located at 865.8 cm^{-1} in the nitrogen matrix and at 866.0 cm^{-1} in the argon matrix. It is assigned to the Si–F(10) + Si–F(11) stretching vibration and the $C(3)H_2$ rocking vibration.

Table 3. Assignment of the infrared absorption spectral bands of matrix isolated cyclohexyltrifluorosilane based on the results of B3LYP/cc-pVTZ anharmonic calculations for the equatorial conformer of the title compound.

Experimental				Calculated anharmonic		Vibrational mode automatic relevance determination (VMARD)	Approximate assignment
N_2 matrix		Ar matrix		B3LYP cc-pVTZ			
ν, cm^{-1}	I, arb. u.	ν, cm^{-1}	I, arb. u.	ν, cm^{-1}	I, arb. u.		
				2966.6	20.0	17.3%S10 + 12.1%S6 +12.0%S12 + 11.2%S9 + 9.3%S3 + 9.2%S16	$\nu_s C(2)H_2 + \nu_s C(3)H_2 + \nu_s C(4)H_2$
2949.8	4.3	2950.0	13.0				
2945.5	19.1	2943.5	18.2	2938.6	39.3	14.4%S4 + 14.0%S15	$\nu_{as} CH_2$
2940.1	14.2	2938.3	16.9	2935.8	3.2	16.5%S13 + 16.3%S7 + 12.6%S15 + 12.3%S4	$\nu_{as} C(1)H_2 + \nu_{as} C(2)H_2 + \nu_{as} C(3)H_2 + \nu_{as} C(4)H_2 + \nu_{as} C(5)H_2$
2934.1	9.3	2931.8	11.7	2923.8	50.6	25.0%S4 + 24.9%S15 + 11.2%S3 + 10.9%S16	$\nu_{as} C(5)H_2 + \nu_{as} C(1)H_2$
2919.8	1.2	2918.9	1.3	2923.1	10.8	27.9%S13 + 27.6%S7 + 9.8%S6 + 9.7%S12	$\nu_{as} C(2)H_2 + \nu_{as} C(4)H_2$
2910.2	2.5	2908.1	3.9	2897.6	12.5	38.4%S9 + 13.7%S7 + 13.7%S13 + 9.8%S10	$\nu_{as} C(2)H_2 + \nu_{as} C(3)H_2 + \nu_{as} C(4)H_2$
2878.3	1.2	2870.3	6.5	2868.6	10.6	18.0%S16 + 17.9%S3 + 9.4%S15 + 9.4%S4 + 9.1%S12	$\nu_s C(1)H_2 + \nu_s C(4)H_2 + \nu_s C(5)H_2$
2868.7	7.4	2865.1	10.4	2867.3	8.4	15.9%S16 + 15.7%S3 + 9.5%S15 + 9.4%S4	$\nu_s C(1)H_2 + \nu_s C(3)H_2 + \nu_s C(5)H_2$
2863.9	12.4	2860.8	10.4				
				2833.9	8.9	21.9%S6 + 21.6%S12 + 13.2%S16 + 12.9%S3	$\nu_s C(1)H_2 + \nu_s C(2)H_2 + \nu_s C(4)H_2 +$
				2830.9	15.9	61.9%S17 + 11.9%S3 + 11.8%S16	$\nu C(6)H$
				2822.7	4.3	31.6%S10 + 20.1%S6 + 20.1%S12	$\nu_s C(2)H_2 + \nu_s C(3)H_2 + \nu_s C(4)H_2 +$
1467.1	0.6	1465.5	1.3	1477.1	3.6	17.5%S33 + 17.4%S56 + 15.9%S45 + 11.9%S39 + 11.8%S51	sc CH_2
1460.9	0.6	1459.8	1.3	1465.7	0.9	27.4%S56 + 25.6%S33 + 11.6%S51 + 11.1%S39	sc $C(1)H_2$ + sc $C(2)H_2$ + sc $C(4)H_2$ + sc $C(5)H_2$
1453.0	11.7	1453.2	13.0	1456.9	1.5	23.4%S39 + 23.3%S51 + 14.8%S56 + 14.8%S33	sc $C(2)H_2$ + sc $C(4)H_2$ + sc $C(5)H_2$
1448.6	1.9	1448.6	5.2	1440.9	4.3	27.5%S45 + 10.9%S33	sc $C(3)H_2$ + sc $C(1)H_2$
				1435.9	1.5	16.8%S51 + 15.8%S39	sc $C(4)H_2$ + sc $C(2)H_2$

Table 3. (Continued)

Experimental				Calculated anharmonic		Vibrational mode automatic relevance determination (VMARD)	Approximate assignment
N_2 matrix		Ar matrix		B3LYP cc-pVTZ			
ν, cm^{-1}	I, arb. u.	ν, cm^{-1}	I, arb. u.	ν, cm^{-1}	I, arb. u.		
1365.4	1.9	1364.8	1.3	1364.1	1.6	6.6%S29	ω C(1)H_2
				1349.3	0.3	5.7%S34	ω C(2)H_2 + ω C(4)H_2
				1347.1	0.1	8.3%S41	ω C(3)H_2
1330.9	0.6	1330.7	1.3	1334.6	0.3	7.6%S43	ω C(2)H_2 + ω C(4)H_2
				1332.1	0.2	7.1%S53	ω CH_2
1302.6	0.6	1302.2	1.3				
1298.8	0.6	1297.6	1.3	1297.2	0.1	7.9%S54	δ C-CH_2
1283.9	1.2	1283.9	2.6	1277.0	1.2	6.3%S52	tw C(1)H_2 + tw C(5)H_2
1275.9	8.0	1276.1	10.4	1268.4	5.8	7.6%S43	tw C(2)H_2 + tw C(4)H_2
				1258.3	0.2	7.4%S25	tw C(3)H_2
1203.7	9.3	1202.8	11.7	1201.6	4.0	9.2%S57	δ Si-C(6)-H
1176.8	2.5	1177.1	3.9	1173.3	1.2	7.0%S27	tw C(2)H_2 + tw C(4)H_2
1116.4	3.7	1116.3	7.8	1106.9	4.6	5.8%S18	δ (ring) C-C
1113.8	5.6	1113.4	7.8				
1111.3	10.5	1111.4	9.1				
1089.1	0.6	1088.7	1.3				
1076.9	0.6	1075.7	1.3	1073.2	2.1	5.6%S24	τ CH_2
1075.0	2.5	1074.3	1.3				
				1055.8	0.6	11.6%S5 + 11.6%S8 + 10.9%S11 + 10.9%S1	ν_{as} (ring) CC
1039.8	3.7	1039.5	2.6	1022.5	1.78	13.5%S2 + 13.5%S14	ν C(1)-C(6) + ν C(5)-C(6)
1030.9	0.6	1030.5	1.3	1014.8	1.1	9.7%S1 + 9.6%S11	ν C(1)-C(2) + ν C(4)-C(5)
1026.5	3.7	1025.9	1.3				
1022.5	6.8	1023.3	9.1				
1008.6	23.5	1008.6	31.2	996.8	6.2	5.0%S11	ν C(4)-C(5)
961.0	4.3	962.7	87.0	936.1	100.0	35.1%S21 + 35.0%S20	ν Si-F(10) + ν Si-F(11)
957.8	100.0	960.8	100.0				
950.9	75.9	952.7	97.4	929.8	83.1	37.4%S19 + 17.1%S21 + 16.9%S20	ν Si-F(9) + ν Si-F(10) + ν Si-F(11)
948.2	25.9	948.6	9.1				
945.1	9.9	945.5	9.1				
937.1	3.7	939.0	6.5				
				908.9	0.1	8.4%S42	ρ CH_2
909.1	20.4	908.7	66.2	886.8	74.6	10.7%S18	ν Si-C(6)
906.9	67.9	906.2	19.5				
902.2^{sh}	9.9	900.6^{sh}	15.6				
886.9	4.3	885.1	3.9	871.3	3.3	12.4%S1 + 12.2%S11	ν C(1)-C(2) + ν C(4)-C(5)
871.1	5.6	871.7	10.4	859.2	34.9	11.6%S20 + 11.5%S21	ν Si-F(10) + ν Si-F(11) + ρ C(3)H_2
865.8	41.4	866.0	70.1				

Table 3. (Continued)

Experimental				Calculated anharmonic		Vibrational mode automatic relevance determination (VMARD)	Approximate assignment
N_2 matrix		Ar matrix		B3LYP cc-pVTZ			
ν, cm^{-1}	I, arb. u.	ν, cm^{-1}	I, arb. u.	ν, cm^{-1}	I, arb. u.		
854.9	3.1	854.2	6.5				
845.3	3.1	844.7	5.2				
				829.1	2.7	9.8%S5 + 9.8%S8	ρ C(3)H_2 + δ C(4)-C(3)-C(2)
808.4	19.1	809.7	11.7	790.2	10.2	9.2%S8	ν (ring breathing)
805.9	1.2	807.9	11.7	784.1	0.3	6.3%S14	ν_{as} (ring) C-C + ρ CH_2
719.6	1.2	720.1	2.6	704.4	2.8	13.1%S19 + 10.8%S18	δ C(5)-C(6)-C(1) + ρ CH_2
588.5	1.2	588.7	1.3				
				517.9	11.1	2.9%S90	ρ CH_2

Notes: br, broad; sh, shoulder; ν, stretching; ν_s, symmetric stretching; ν_{as}, asymmetric stretching vibrations; δ, bending in plane deformation; γ, bending out of plane deformation; ρ, rocking; ω, wagging; τ, twisting; sc, scissoring; arb. u., arbitrary units.

Another range with an intense spectral band is located at 3000–2800 cm^{-1}. This region includes vibrational modes that can be assigned to various CH_2 symmetric and asymmetric stretching vibrations.

The good agreement between the calculated IR absorption spectrum and the matrix isolated spectrum of cyclohexyltrifluorosilane confirms the computational result that, under real conditions, the substance exists only as a single conformer – the chair equatorial form.

4. Conclusions

Using anharmonic frequency calculations at the DFT/B3LYP/cc-pVTZ level of theory assignment of experimental spectral bands in the fingerprint spectral region was performed. Based on the detailed theoretical analysis of the conformational landscape of the cyclohexyltrifluorosilane molecule, two possible conformers were found: a global minimum structure with chair equatorial conformation and a local minimum structure with chair axial conformation. The relative energy difference was calculated to be 6.3 kJ/mol and the energy barrier for an interconversion via ring inversion from chair axial to chair equatorial was 18.9 kJ/mol, making this process unfavoured under the experimental conditions. Calculations of the relative abundance of both conformers taking into account the Boltzmann distribution at 300 K reveal that the population ratio is approximately 1:12, with one chair axial molecule for every 12 chair equatorial molecules what makes the chair axial conformer unobservable in the matrix spectra.

Acknowledgements

Authors are thankful for the provided computational time at the High Performance Computing Center (HPCC) of the Lithuanian National Center of Physical and Technology Sciences (NCPTS) at Physics Faculty of Vilnius University.

References

[1] S.J. Clarson, J.J. Fitzgerald, M.J. Owen, S.D. Smith, and M.E. Van Dyke, *Advances in Silicones and Silicone-modified Materials*, ACS Symposium Series, Vol. 1051 (American Chemical Society, WA, 2010).

[2] J.P. Blitz and C.B. Little, *Fundamental and Applied Aspects of Chemically Modified Surfaces* (The Royal Society of Chemistry, 1999).

[3] J. El-Maiss, T. Darmanin, E.T. de Givenchy, S. Amigoni, J. Eastoe, M. Sagisaka, and F. Guittard, Superhydrophobic surfaces with low and high adhesion made from mixed (hydrocarbon and fluorocarbon) 3,4-propylenedioxythiophene monomers, J. Polym. Sci. B **52**(11), 782–788 (2014), https://doi.org/10.1002/polb.23483

[4] E. Juaristi, *Introduction to Stereochemistry and Conformational Analysis* (John Wiley and Sons, New York, 1991).

[5] H.A. Taha, M.R. Richards, and T.L. Lowary, Conformational analysis of furanoside-containing mono- and oligosaccharides, Chem. Rev. **113**, 1851 (2013), https://doi.org/10.1021/cr300249c

[6] K. Nester, K. Gaweda, and W. Plazinski, A GROMOS force field for furanose-based carbohydrates, J. Chem. Theory Comput. **15**, 1168 (2019), https://doi.org/10.1021/acs.jctc.8b00838

[7] A.R. Ionescu, A. Bérces, M.Z. Zgierski, D.M. Whitfield, and T. Nukada, Conformational pathways of saturated six-membered rings. A static and dynamical density functional study, J. Phys. Chem. A **109**(36), 8096–8105 (2005), https://doi.org/10.1021/jp052197t

[8] T.M.C. McFadden, R. Platakyte, J. Stocka, J. Ceponkus, V. Aleksa, T. Carrigan-Broda, V. Sablinskas, P. Rodziewicz, and G.A. Guirgis, Experimental (Raman and IR) and computational (DFT, MP2) studies of conformational diversity of 1-chloromethyl-1-fluorosilacyclohexane, J. Mol. Struct. **1221**, 128786 (2020), https://doi.org/10.1016/j.molstruc.2020.128786

[9] J. Stocka, R. Platakyte, T.M.C. McFadden, J. Ceponkus, V. Aleksa, A.G. Hanna, V. Sablinskas, P. Rodziewicz, and G.A. Guirgis, Conformational diversity of 1-chloro-1-chloromethylsilacyclohexane with experimental (Raman and IR) and computational (DFT, MP2) methods, J. Mol. Struct. **1249**, 131644 (2022), https://doi.org/10.1016/j.molstruc.2021.131644

[10] J.C.P. Schwarz, Rules for conformation nomenclature for five- and six-membered rings in monosaccharides and their derivatives, J. Chem. Soc. Chem. Commun. **14**, 505–508 (1973), https://doi.org/10.1039/C39730000505

[11] A.V. Belyakov, Y. Sigolaev, S.A. Shlykov, S.Ó. Wallevik, N.R. Jonsdottir, R. Bjornsson, S. Jonsdottir, Á. Kvaran, T. Kern, K. Hassler, and I. Arnason, Conformational properties of 1-*tert*-butyl-1-silacyclohexane, $C_5H10SiH(t\text{-}Bu)$: Gas-phase electron diffraction, temperature-dependent Raman spectroscopy, and quantum chemical calculations, Struct. Chem. **26**, 445–453 (2014), https://doi.org/10.1007/s11224-014-0503-6

[12] A.D. Becke, Density-functional thermochemistry. III. The role of exact exchange, J. Chem. Phys. **98**, 5648–5652 (1993), https://doi.org/10.1063/1.464913

[13] T.H. Dunning Jr., Gaussian basis sets for use in correlated molecular calculations. I. The atoms boron through neon and hydrogen, J. Chem. Phys. **90**, 1007–1023 (1989), https://doi.org/10.1063/1.456153

[14] S. Grimme, J. Antony, S. Ehrlich, and H. Krieg, A consistent and accurate *ab initio* parametrization of density functional dispersion correction (DFT-D) for the 94 elements H-Pu, J. Chem. Phys. **132**, 154104 (2010), https://doi.org/10.1063/1.3382344

[15] F. Teixeira, M. Natália, and D.S. Cordeiro, Improving vibrational mode interpretation using Bayesian regression, J. Chem. Theory Comput. **15**(1), 456–470 (2019), https://doi.org/10.1021/acs.jctc.8b00439

EKSPERIMENTINIAI (RAMANO IR IR SPEKTROSKOPINIAI) IR SKAIČIUOJAMIEJI (TANKIO FUNKCIONALO METODU) CIKLOHEKSILTRIFLUOROSILANO TYRIMAI

J. Mačytė [a], J. Lach [a], M. Gregory [b], S. Gordon [b], J. Čeponkus [a], V. Šablinskas [a], G.A. Guirgis [b]

[a] *Vilniaus universiteto Fizikos fakultetas, Vilnius, Lietuva*

[b] *Čarlstono koledžo Chemijos ir biochemijos katedra, Čarlstonas, JAV*

Santrauka

Šiame darbe pristatomas naujai susintetinto cikloheksiltrifluorosilano tyrimas, taikant virpesinę spektroskopiją (Ramano sklaidos ir IR spektroskopijos) bei teorinius skaičiavimus tankio funkcionalo (DFT) teoriniame artinyje. Tyrimo tikslas – nustatyti stabilias šio molekulinio junginio struktūras ir priskirti eksperimentines virpesines spektrines juostas. Skaičiavimai prognozuoja dviejų stabilių „kėdės“ konformacijų egzistavimą: „kėdės“ ekvatorinės (energiškai palankiausios) ir „kėdės“ ašinės. Šių konformacijų potencinės energijos skirtumas yra 6,3 kJ/mol, o konformacinės konversijos barjeras – 18,9 kJ/mol. Toks konversijos barjeras yra per aukštas, kad vyktų konformaciniai virsmai matricinių eksperimentų sąlygomis. Siekiant visapusiškai priskirti junginio virpesines spektrines juostas normaliesiems virpesiams, buvo panaudoti ATR-FTIR, Ramano sklaidos ir matricinės izoliacijos IR spektroskopijos eksperimentiniai duomenys kartu su DFT skaičiavimais. Eksperimentiniai spektrinių tyrimų rezultatai patvirtina, kad tiriamoje sistemoje egzistuoja tik viena stabili konformacija, t. y. „kėdės“ ekvatorinė.